

Classification of live, untethered zooplankton from observations of multiple-angle acoustic scatter

Paul L. D. Roberts^{a)} and Jules S. Jaffe

Marine Physical Lab, Scripps Institution of Oceanography, La Jolla, California 92093-0238

(Received 4 July 2007; revised 13 May 2008; accepted 14 May 2008)

A broadband, multiple-angle acoustic array was used to classify millimeter to centimeter sized live zooplankton in a laboratory tank. Reflections in the frequency range from 1.5 to 2.5 MHz were recorded from untethered 1–4 mm calanoid copepods and 8–12 mm mysids over an angular range of 0°–47°. A synchronized, coregistered video system recorded animal location and orientation. To highlight differences between animals, a frequency correlation matrix was computed from the observed wide-band power spectra of the scattered sound. Significant differences in the slopes and shapes of the eigenvalue spectra of this matrix were found for mysids versus copepods. These results support the idea that broadband, multiple-angle scatter can be used to classify organisms of different sizes and shapes. © 2008 Acoustical Society of America. [DOI: 10.1121/1.2945114]

PACS number(s): 43.30.Sf, 43.30.Ft, 43.60.Fg [KGF]

Pages: 796–802

I. INTRODUCTION

Crustacean zooplankton play a major role in the ocean's ecosystem, so it is important to develop noninvasive methods to measure their abundance and behavior. Instruments deployed in the laboratory and field have measured sound scatter from a wide range of animals (McNaught, 1968; Holliday *et al.*, 1989; Wiebe *et al.*, 1990; Stanton *et al.*, 1998a; Lavery *et al.*, 2002; Lavery *et al.*, 2007). In addition, scattering models and classification algorithms have been formulated (Martin *et al.*, 1996; Stanton *et al.*, 1998b; Lavery *et al.*, 2002; Lawson *et al.*, 2006) with the ultimate goals of quantification of animal size and abundance, identification of different taxa (Holliday *et al.*, 1989; Holliday *et al.*, 2003; McGehee *et al.*, 2004), and measurements of *in situ* behavior (De Robertis *et al.*, 2000; Genin *et al.*, 2005).

The fundamental challenge to achieving these goals arises from the vast diversity of zooplankton in the ocean and the confounding influence of size, shape, orientation, and material properties on acoustic scatter (McGehee, 1998; Martin Traykovski *et al.*, 1998; Warren *et al.*, 2002). Variations of these factors lead to substantial ambiguities in using acoustics to both identify and count animals. Reducing these ambiguities, while retaining a system that is practical for fieldwork, would be of great value.

One potential solution is to observe sound that has been reflected at different angles. In the context of diffraction theory, Jaffe (2006) demonstrated that swim-bladder size could be accurately inferred from multiple-angle acoustic reflections observed from a single fish. Roberts and Jaffe (2007) used numerical methods to demonstrate that individual copepods and euphausiids could be classified using multiple-angle, wide-band reflections. The study indicated that the multiple-angle method was more accurate than other techniques using either narrow- or wide-band sound with a single transceiver.

Here, the multiple-angle technique was applied to two types of marine zooplankton: copepods and mysids. Copepods are an order of crustacean zooplankton (typically 1–4 mm in length) distributed throughout the world's marine and fresh waters. Mysids are common coastal inhabitants similar in size, shape, and composition to euphausiids (typically 5–10 mm in length). Copepods and euphausiids are dominant taxa of marine ecosystems and there is great interest in quantifying their distributions with remote, noninvasive methods.

A laboratory scattering apparatus was constructed to record simultaneous reflections from zooplankton at multiple observation angles. To be compatible with available hardware, eight receivers were evenly spaced on a line, forming a 2-m-long array. The length of the array was chosen so that it could eventually be deployed on an autonomous underwater vehicle (AUV) or glider. The even spacing of receivers sampled the available aperture uniformly. No optimization of receiver position or array length was attempted, but the final geometry was consistent with simulated multiple-angle experiments (Roberts and Jaffe, 2007). During recording of acoustic reflections, two video cameras simultaneously recorded the size, position, and orientation of animals. Multiple-angle observations were analyzed using a correlation matrix approach designed to highlight changes in scattering across the array. Eigenvalue analyses of these matrices demonstrate that, in our laboratory setup, multiple-angle acoustic data can be used to accurately discriminate between copepods and mysids.

II. EXPERIMENTAL METHODS AND DATA PROCESSING

A. Acoustic scattering apparatus

The scattering apparatus consisted of a linear array of ten disk transducers (Panametrics, Waltham, MA). Eight were used as receivers and two as transmitters. All receivers and one transmitter were 19 mm diameter, 2.25 MHz broadband transducers (V305-SU). The other transmitter had a di-

^{a)}Electronic mail: plobert@ucsd.edu

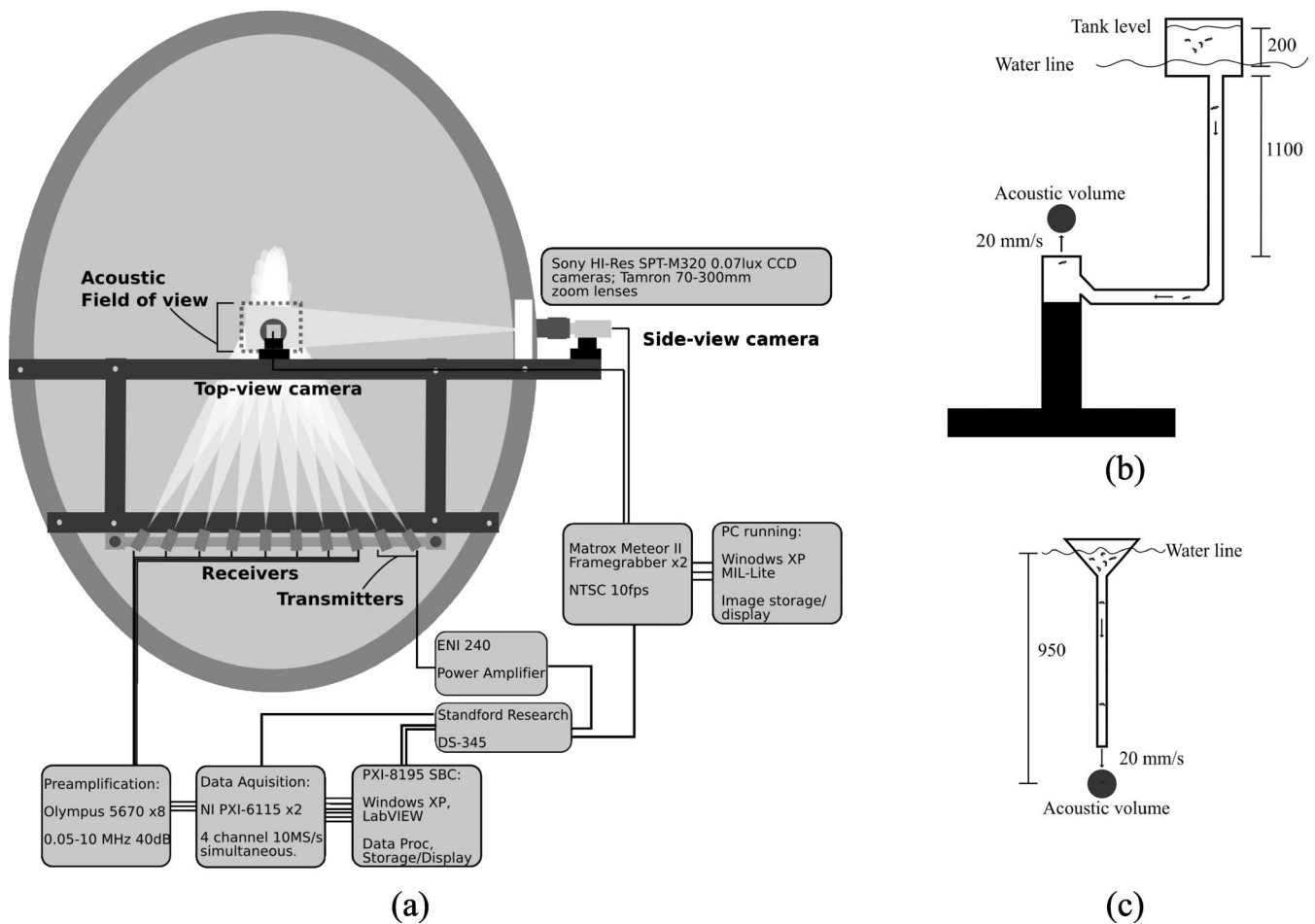


FIG. 1. (a) The multiple-angle scattering apparatus (viewed from above) showing the acoustic and optic elements, Unistrut (Unistrut Corporation) frame, experimental tank, and associated data acquisition components. (b) The bottom-up pump. Animals are drawn out of a tank above the surface and injected below the field of view. (c) The top-down pump. Animals are sedated and allowed to sink through the pipe into the FOV. All distances are in millimeters.

ameter of 38 mm (V395-SU). The larger transmitter was used to increase the source level, improving the signal to noise ratio (SNR) of echoes from smaller animals. The field of view (FOV), defined by the overlap among all acoustic beams, was 42 ml with the 38 mm transmitter and 328 ml with the 19 mm transmitter. Optical images within the FOV were acquired using two, high-sensitivity VGA cameras (Sony SPT-M320). The acoustic array and cameras were rigidly connected by a Unistrut (Unistrut Corporation, Wayne, MI) system to ensure minimal relative movement during experiments [Fig. 1(a)]. A custom-built rail system was used to slide the array in and out of the water. This allowed the array to be kept dry when not being used, and then precisely positioned and locked in place for experiments. All experiments were performed in a 3.0-m-wide, 4.2-m-long, 2.4-m-deep elliptical tank with view ports 1.2 m above the bottom. The tank was filled with chilled, filtered seawater maintained at a temperature of 14.9 °C throughout the experiments.

Acoustic data were acquired by a National Instruments (Austin, TX) PXI-8195 controller running WINDOWS XP (Microsoft, Redmond, WA) with two PXI-6115, 10 MHz, 12 bit, four-channel simultaneous sampling boards with 64 Mbytes of on-board memory. The output from each receiver was fed through a Panametrics 5670 broadband preamplifier prior to digitization. The transmitter was driven by an ENI (Bell

Electronics, Kent, WA) AP400B 400 W power amplifier. Waveforms sent to the power amplifier were generated by a Stanford Research (Sunnyvale, CA) DS345 arbitrary waveform generator. Software developed in LABVIEW (National Instruments) controlled the acquisition, recording, and real-time display of data.

A single personal computer (PC) running WINDOWS 2000 controlled the stereo video system. Images were “grabbed” from each camera—at an adjustable rate controlled by the acoustic transmissions—using synchronized Matrox (Matrox, Dorval, Canada) Meteor II frame grabbers. Software developed in C++ used the Matrox Imaging Library to read images from the boards, bundle them together, display them in real-time, and save them to disk.

To obtain high-contrast images of animals, a 200 mW laser was used for illumination (Aixiz 200 mW, 650 nm module). A wavelength of 650 nm was selected as it is almost invisible to the animals yet suffers limited attenuation through the medium. The laser beam was spread with a diverging lens to yield a cone of light that intersected the FOV.

B. Experimental setup

Preliminary experiments revealed that scatter from tethers maintaining zooplankton in the FOV dominated observa-

tions at these high frequencies. Therefore, a substantial challenge was to position live, untethered animals in the FOV. Copepods were pumped from a small holding tank through a system of hoses and out through a 75 mm diameter pipe positioned directly under the FOV [Fig. 1(b)]. Copepods typically stayed near the FOV for several seconds after exiting the pipe, whereas mysids quickly swam away from the FOV. To mitigate this problem, mysids were sedated by placing them into a dilute (1% by volume) water bath of clove oil and filtered seawater. They were kept in the bath until they ceased swimming (typically 30–60 s) but retained leg movement. Sedated mysids were then transferred immediately to a funnel system [Fig. 1(c)] that guided them into the FOV while they sank slowly. These mysids eventually recovered as inferred by their swimming behavior.

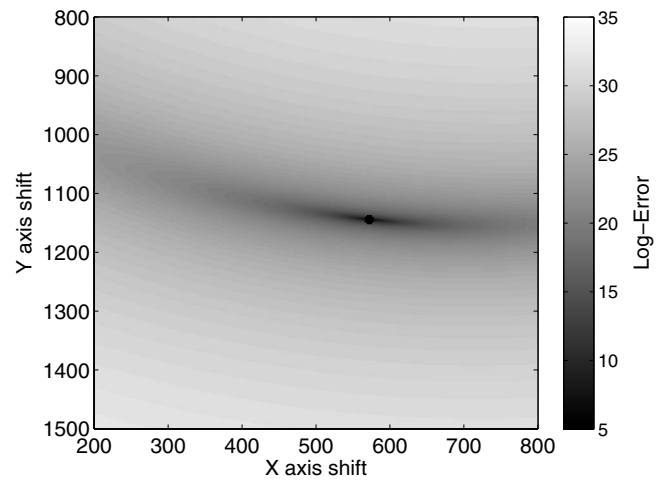
C. System alignment and calibration

Alignment and calibration of the multiple-angle system were more complicated than for a typical monoangle system. Transducers were aligned using a long strand of nylon monofilament suspended perpendicular to the array at a point that was designated the system's origin. The monofilament's diameter of 75 μm resulted in an acoustic scattering pattern that was omnidirectional in the horizontal plane, but narrow in the vertical plane. Pointing angles for all transmitters and receivers were iteratively adjusted to maximize reflections.

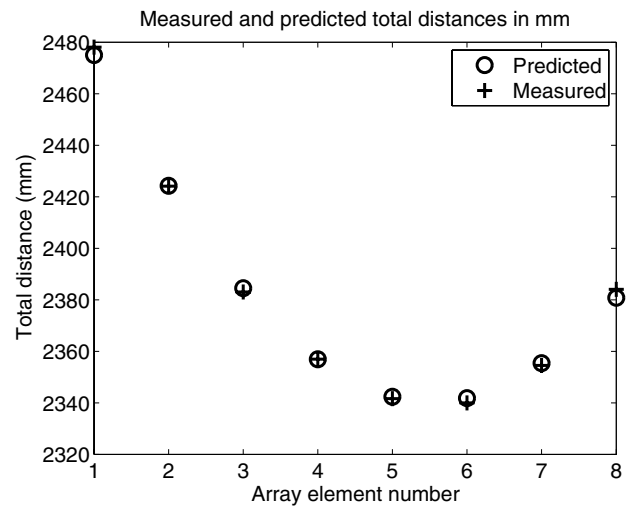
Three-dimensional transducer positions were estimated using the time of arrival at each receiver of the echo scattered from the monofilament. With the array elements located on a line, their Euclidean offsets from the origin were determined by computing the mean square error between the observed and predicted arrival times of echoes at each receiver, for all possible offsets. A clear minimum was found [Fig. 2(a)] and the model output, compared to measured data, yielded excellent agreement [Fig. 2(b)]. The array was off center with a total angular span of roughly 46.7° (Fig. 3). The horizontal distance from the center of the array to the origin was 1.14 m and the angular spacing between array elements was on average $5.8^\circ \pm 1^\circ$.

The video system was aligned with the acoustic system using a small sphere suspended in the middle of the FOV. One camera was mounted so that it looked through the tank's view port (side view). The second camera was mounted in a waterproof housing with a small view port and submerged almost directly above the FOV (top view). Both cameras were mounted to the Unistrut frame using heavy-duty, three-axis telescope mounts (Losmandy DCM2, Los Angeles, CA). These mounts allowed each camera to be rotated until the target was in the center of each frame. They were then locked in place.

Before and after experiments, acoustic calibrations were performed using a 1 mm diameter tungsten carbide sphere, following the calibration procedure outlined by Foote (1990). Echoes were collected while the sphere was translated within the FOV. Since the echo spectrum varied only slightly for displacements of the sphere within the FOV, the beam pattern was assumed to be constant in that region. The echo spectrum from the sphere was then used to convert



(a)



(b)

FIG. 2. Calibration results for the array. (a) The error surface for the x and y shift parameters using the calibration data, the inferred sound speed, and the measured element spacing. (b) The modeled and measured total acoustic path distances for each receiver. The total acoustic path is the path from the transmitter, to the origin, and then to the receiver.

recorded echo spectra to target strength. This process was repeated with the nylon monofilament using the scattering model described by Minonzo *et al.* (2005). To check consistency of the calibration, echo spectra—converted to target strength using each calibration method—were compared and found to be within 3 dB. This was adequate for the subsequent analyses as the method only relies on the relative calibration among receivers.

D. Data acquisition and processing

Multiple-angle data were collected during a series of experiments spanning several months. All zooplankton were collected in the La Jolla Cove area (San Diego, CA) by small boat and immediately brought back to the laboratory. Mysids were collected by gently dragging a mesh butterfly net across the kelp at the surface of the kelp forest. This procedure typically resulted in 10–100 mysids ranging from length

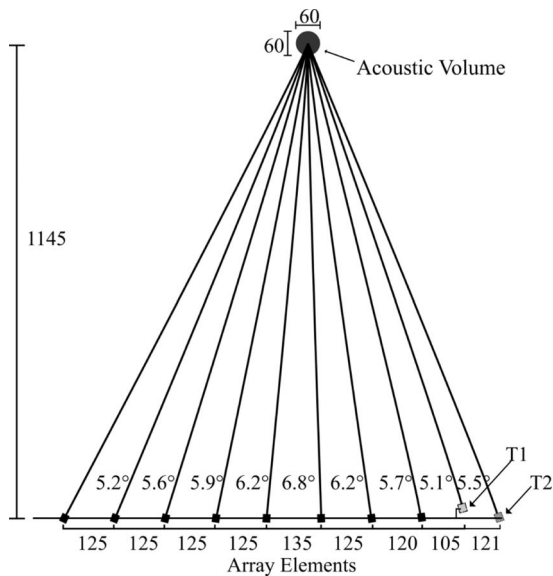


FIG. 3. The geometry of the acoustic array. All distances are in millimeters. The two transmitters are at the right end of the array. Receiver element 1 is at the left end of the array and element 8 is at the right end of the array.

8 to 12 mm. Copepods were collected in a series of net tows using a 250 μm cod end, 1 m diameter net. This yielded several thousand copepods (primarily calanoid) ranging in length from 1 to 4 mm. Animals were allowed to equilibrate with seawater siphoned directly from the FOV for 30 min prior to being injected into the tank. During experiments, between one and ten copepods were injected toward the FOV at a time. Only one mysid was injected at a time. Of those animals injected, roughly 10% actually passed through the FOV.

The transmit signal was a linear frequency-modulated (LFM) chirp from 1.5 to 2.5 MHz with a cosine-squared envelope and a duration of 500 μs . The data-acquisition system recorded ten sequential echoes with 100 ms delay between them. The large tank and relatively small volume of intersection between transmitter and receivers allowed a nearly reverberation-free echo. However, in data from the mysid experiments, there were some small artifacts caused by the injection pipe. These were coherently removed in postprocessing using data recorded from the pipe alone.

Raw acoustic data were matched filtered with a synthetic model of the transmit signal (Chu and Stanton, 1998; Kay, 1998; Warren *et al.*, 2002). The matched-filter output was then windowed to localize the echo from the animal. A window length of 250 time samples (25 μs at 10 MHz sample rate) was selected to capture the longest possible echo for the largest animal insonified. Due to the extended length of the transmit signal, the matched-filter processing gave a SNR improvement of roughly 23 dB over a very short pulse of equivalent power. This processing gain was critical for obtaining good SNR from these weakly scattering animals. The same matched filter was also applied to calibration data. A 4800-point fast Fourier transform (FFT) was used to estimate power spectra of echoes recorded by each receiver. The FFT of each received echo was multiplied by the power spectrum predicted by the calibration model and divided by the power

spectrum of the calibration echo. This corrected for the shape of the transmit pulse and the small variation in element sensitivity across the array.

To highlight fundamental differences between echoes from each class of scatterers, a frequency correlation algorithm was developed. Let the M -point FFT of the windowed, matched-filter output for the j th element be $F_j[k]$. Then define the cross correlation between the positive frequency coefficients of the FFTs of two elements a and b as

$$X_{a,b}[m] = \sum_{k=0}^{k=N} F_a^H[((k))_N] F_b[((k-m))_N]$$

for $1 \leq a \leq 8$ and $1 \leq b \leq 8$, (1)

where $((x))_N$ denotes $x \bmod N$ and $N=(M+2)/2$. The cross correlation with the maximum magnitude was then used to form an approximately Hermitian, positive-semidefinite matrix

$$G_{a,b} = X_{a,b}[m^*], \quad (2)$$

where

$$m^* = \arg \max_m |X_{a,b}[m]|. \quad (3)$$

As explained in Roberts and Jaffe (2007), the matrix G will be nearly rank 1 if there is an equal correlation between all pairs of receivers. In contrast, if there is a weak correlation between nonidentical pairs of receivers G will be similar to a scaled identity matrix.

To quantify the degree of correlation, the eigenvalue decomposition (Moon and Stirling, 2000) was computed as

$$\Lambda = Q^H G Q, \quad (4)$$

where $\Lambda = \text{Diag}(\lambda_1, \dots, \lambda_8)$ is a diagonal matrix of eigenvalues. In practice, there was a substantial amount of correlation among echoes across the array, and the eigenvalues decreased logarithmically. Therefore, the log-eigenvalue spectrum was used for analysis.

III. RESULTS

A. Scattering apparatus and experiment analysis

The transducer array, video system, and data-acquisition hardware worked well for collecting repeatable, multiple-angle scattering measurements when animals were positioned in the FOV. The combination of a rigid frame, with robust rotation mounts for all sensors, allowed simple and straightforward alignment that remained unchanged throughout the experiments. The rail system for translating the array in and out of the water proved invaluable and was constructed using standard, off-the-shelf parts at small cost. The camera system's low resolution, coupled with the interlaced video signal and poor laser-beam characteristics, yielded images of only moderate quality, though they were adequate for this study.

Positioning live specimens in the FOV without causing artifacts in recorded data was the most challenging aspect of these experiments. Numerous methods were evaluated during the development of the system (including a wide variety

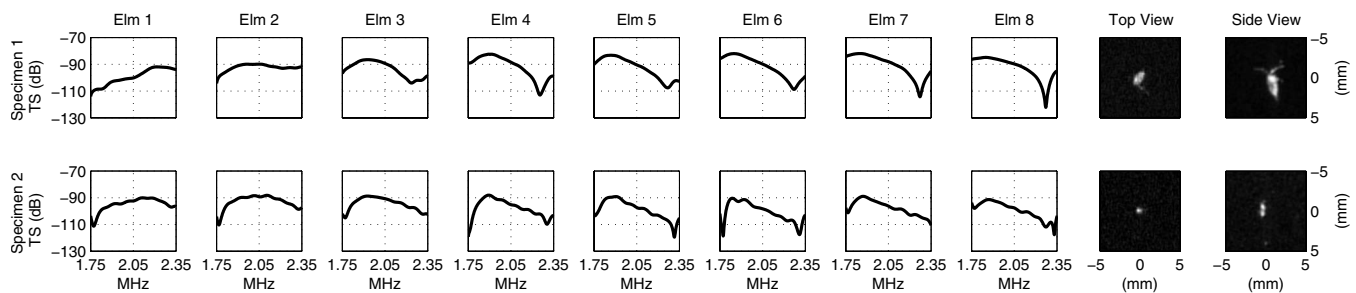


FIG. 4. Example data for two different copepods. Data are plotted for each receiver elements 1–8 as calibrated target strength vs frequency. Images on the far right show top and side views of the copepods at the time of insonification. These images are oriented so that the array is at the bottom of the top-view image with element 1 on the left. For the side-view image, element 1 is oriented into the page, and element 8 is out of the page.

of tethers) but the injection method provided the only artifact-free data. Unfortunately, the injection frequently added bubbles to the acoustic field, or the animal would move out of the FOV before reflections were recorded. Therefore, few artifact-free echoes were obtained during experiments. Data are presented here from eight individual copepods and eight individual mysids. The small size of the data set is solely a consequence of the lack of an efficient means for repeatedly placing untethered, live animals in the FOV.

B. Multiple-angle data analysis

Multiple-angle data require additional processing to characterize target animals. In the first step, spectra of echoes at each angle were computed (Figs. 4 and 5). Despite the small sample size, patterns in target strength data were clear. These highlighted the influence of animal orientation on echo spectra, motivating the frequency correlation processing.

For copepods, target strength curves (Fig. 4) were very similar among receivers. In addition, target strength was slowly varying across frequencies. Video observations indicated that both specimens shown in Fig. 4 were nearly broadside to the array. However, a small tilt can be inferred from a null in power spectra moving from elements 1–8. Multiple-angle data can therefore offer enhanced insight into the animal's orientation.

For mysids, target strength is less similar among receivers than with copepods, and varies more as a function of frequency (Fig. 5). Video data showed that, for the two specimens shown in Fig. 5, orientation in the horizontal plane differed by roughly 90° (Fig. 5, top-view images).

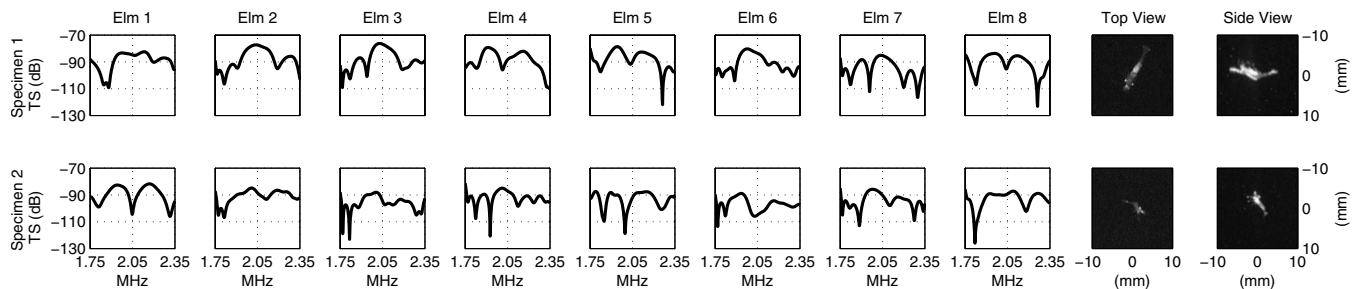


FIG. 5. Example data for two different mysids. Data are plotted for each receiver elements 1–8 as calibrated target strength vs frequency. Images on the far right show top and side views of the copepods at the time of insonification. Images are oriented identical to Fig. 4. Note that the image scale is changed from Fig. 4.

Specimen 1 was nearly end on to element 1 and nearly broadside to element 8. Specimen 2 was nearly broadside to element 1 and nearly end on to element 8. Orientations can also be inferred from acoustic data: there is a decrease in spectral complexity as the animal orientation becomes closer to broadside. Near broadside, spectra are smoother with a well-defined null. This null is likely a result of interference between sound reflected from the sides of the mysid's body closest to and farthest from the array element.

To highlight differences among data sets, multiple-angle spectra for each specimen were combined together to form an image. The spectrum for each angle was first normalized by its standard deviation to remove relative differences in the average reflected energy. When plotted as a function of frequency and angle (Fig. 6), this normalized spectral magnitude shows substantial similarity among frequency and angle for copepods [Fig. 6(a)] with more variability for mysids [Fig. 6(b)].

Frequency correlations among spectra of angular data were computed using Eqs. (1) and (2). Log-eigenvalue spectra (Fig. 7) indicate that echoes at each angle are more correlated for copepods than for mysids: the slope of the average spectrum for copepods is roughly twice that for mysids. Furthermore, the average spectrum for copepods decreases steadily, whereas for mysids it is rather flat up to the sixth eigenvalue at which point it steadily decreases.

IV. DISCUSSION AND CONCLUSIONS

Experiments using a multiple-angle acoustic receiver array and live copepods and mysids have shown that it is possible to use the scattered acoustic signal to distinguish between these zooplanktonic taxa. Preliminary experiments

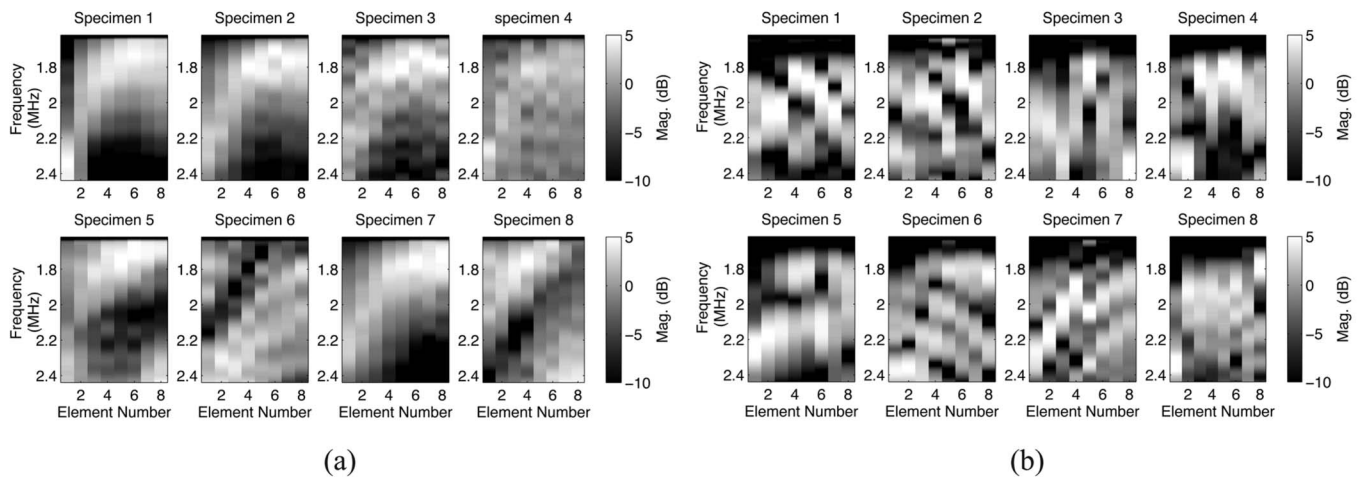


FIG. 6. (a) Normalized magnitude of the scattering spectrum as a function of frequency and array element number for all eight copepod specimens. These data highlight the slowly varying nature of target strength as a function of frequency and look angle. (b) Normalized magnitude of the scattering spectrum as a function of frequency and element number for all eight mysid specimens. These data highlight the relative increase in complexity of target strength as a function of frequency and look angle when compared to (a).

showed that signals from animals tethered in the FOV were dominated by scatter from the tether. Techniques were developed to introduce live, untethered animals into the FOV; however, data quantity was limited by the low success rate in positioning animals in the FOV. In a real pelagic environment these factors would not be an issue.

Multiple-angle data (Figs. 4–6) exemplify a fundamental principle of sound scattering from weak scatterers: the scattered sound field in the immediate vicinity of a target and its radiated pattern in the far field are Fourier transform pairs (Morse and Ingard, 1968). Therefore, variability in target strength is controlled by the size and shape of the scatterer. A thicker scatterer at a given orientation permits more variability over frequency for a fixed bandwidth. Likewise, a more elongate scatterer permits more variability over angle. This can complicate the interpretation of single-angle, wide-band scatter when animal orientation is unknown (Martin Traykovski *et al.*, 1998). A comparison of data from single angles (Fig. 6) reveals that single broadband echoes from copepods

and mysids can be quite similar depending on the orientation of the animal relative to the system. However, when multiple angles are considered, this similarity is dramatically reduced.

A further advantage of the method presented here is that transducers only need to be intercalibrated and not absolutely calibrated. This method is therefore relatively immune to biofouling, so long as the biofouling occurs equally for all array elements. A potential disadvantage is that multiple elements require more sophisticated hardware and computer processing than a single-element system. However, several existing systems use multiple transducer configurations for measuring Doppler shifts to infer currents, so this is not a problem—even in a battery-powered instrument. Furthermore, the computational burden is modest.

While this study has demonstrated the utility of a multiple-angle array for zooplankton identification, there remain several research issues requiring further consideration. One concerns optimizing the array geometry: the number of elements, the distance between them, and the overall length of the array. Another concerns extension of the processing methods, once the data are in hand. The eigenvalue method described here works well in analyzing the presented laboratory data; however, alternate analyses should be explored.

Naturally, the real challenge in zooplankton sensing is to implement the method in the ocean. Beyond the basic issue of putting electronic instruments in a corrosive, high-pressure environment, there is the added problem of the large diversity of animals: the many compositional types and body morphologies make enumeration and identification difficult. One approach might be to combine the use of broadband, multiple-angle scattered sound with target-strength observations of individuals. Such a system would generate information about both the size and reflectivity of the animals, with reduced sensitivity to their absolute orientation. This will greatly reduce the number of candidate animals corresponding to a measured set of reflections, enhancing our ability to discriminate among them. Incorporating these ideas into a sea-going system will increase our knowledge about the ma-

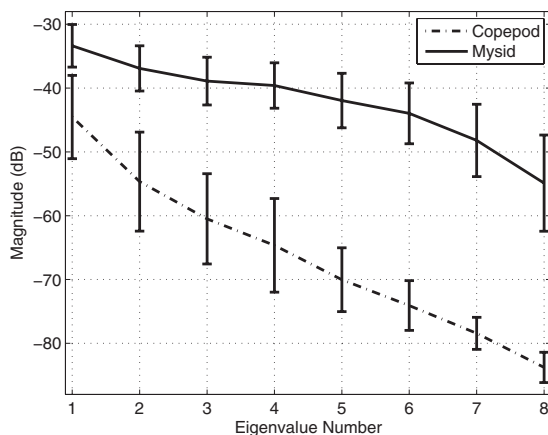


FIG. 7. Average log-eigenvalue spectrum for copepod (dashed) and mysid (solid) data. Error bars denote one standard deviation. The slope of the log-eigenvalue spectrum for copepods is roughly twice that for mysids demonstrating a greater degree of correlation among echoes at each angle for copepods.

rine planktonic ecosystem and the role of zooplankton in the regulating the dynamics and fluxes through that ecosystem.

ACKNOWLEDGMENTS

The authors would like to thank the SIO machine shop for assistance with construction of the scattering apparatus, Eddie Kisfaludy, Erdem Karakoylu, Fernando Simonet, Ben Maurer, and Robert Glatts for technical consulting on the scattering apparatus design and help with experiments, two anonymous reviewers and Peter Franks for helpful comments on the manuscript, and the California Sea Grant for funding this research.

- Chu, D. Z., and Stanton, T. K. (1998). "Application of pulse compression techniques to broadband acoustic scattering by live individual zooplankton," *J. Acoust. Soc. Am.* **104**, 39–55.
- De Robertis, A., Jaffe, J. S., and Ohman, M. D. (2000). "Size-dependent visual predation risk and the timing of vertical migration in zooplankton," *Limnol. Oceanogr.* **45**, 838–1844.
- Footte, K. G. (1990). "Spheres for calibrating an 11-frequency acoustic measurement system," *ICES J. Mar. Sci.* **46**, 284–286.
- Genin, A., Jaffe, J. S., Reef, R., Richter, C., and Franks, P. J. S. (2005). "Swimming Against the Flow: a Mechanism of Zooplankton Aggregation," *Science* **308**, 860–862.
- Holliday, D. V., Donaghay, P. L., Greenlaw, C. F., McGehee, D. E., McManus, M. M., Sullivan, J. M., and Miksis, J. L. (2003). "Advances in defining fine- and micro-scale pattern in marine plankton," *Aquat. Living Resour.* **16**, 131–136.
- Holliday, D. V., Pieper, R. E., and Kleppel, G. S. (1989). "Determination of zooplankton size and distribution with multi-frequency acoustic technology," *ICES J. Mar. Sci.* **46**, 51–62.
- Jaffe, J. S. (2006). "Using multiple-angle scattered sound to size fish swim bladders," *ICES J. Mar. Sci.* **63**, 1397–1404.
- Kay, S. M. (1998). *Fundamentals of Statistical Signal Processing: Detection Theory* (Prentice-Hall, Upper Saddle River, NJ), Vol. 2.
- Lavery, A. C., Stanton, T. K., McGehee, D. E., and Chu, D. Z. (2002). "Three-dimensional modeling of acoustic backscattering from fluid-like zooplankton," *J. Acoust. Soc. Am.* **111**, 1197–1210.
- Lavery, A. C., Wiebe, P. H., Stanton, T. K., Lawson, G. L., Benfield, M. C., and Copley, N. (2007). "Determining dominant scatterers of sound in mixed zooplankton populations," *J. Acoust. Soc. Am.* **122**, 3304–3326.
- Lawson, G. L., Wiebe, P. H., Ashjian, C. J., Chu, D. Z., and Stanton, T. K. (2006). "Improved parameterization of Antarctic krill target strength models," *J. Acoust. Soc. Am.* **119**, 232–242.
- Martin, L. V., Stanton, T. K., Wiebe, T. K., and Lynch, J. F. (1996). "Acoustic classification of zooplankton," *ICES J. Mar. Sci.* **53**, 217–224.
- Martin Traykovski, L. V., O'Driscoll, R. L., and McGehee, D. E. (1998). "Effect of orientation on broadband acoustic scattering of Antarctic Krill *Euphausia superba*: Implications for inverting zooplankton spectral signatures for angle of orientation," *J. Acoust. Soc. Am.* **104**, 2121–2135.
- McGehee, D. E., Demer, D. E., and Warren, J. D. (2004). "Zooplankton in the Ligurian Sea: Part I. Characterization of their dispersion, relative abundance and environment during summer 1999," *J. Plankton Res.* **26**, 1409–1418.
- McGehee, D. E., O'Driscoll, R. L., and Traykovski, L. V. M. (1998). "Effects of orientation on acoustic scattering from Antarctic krill at 120 kHz," *Deep-Sea Res., Part II* **45**, 1273–1294.
- McNaught, D. C. (1968). "Acoustical determination of zooplankton distributions," in *The 11th Annual Conference on Great Lakes Research*, pp. 76–84.
- Minonzio, J. G., Prada, C., Chambers, D., Clorennec, D., and Fink, M. (2005). "Characterization of subwavelength elastic cylinders with the decomposition of the time-reversal operator: Theory and experiment," *J. Acoust. Soc. Am.* **117**, 789–798.
- Moon, T. K., and Stirling, W. C. (2000). *Mathematical Methods and Algorithms for Signal Processing* (Prentice-Hall, Upper Saddle River, NJ).
- Morse, P. M., and Ingard, K. U. (1968). *Theoretical Acoustics* (Princeton University Press, Princeton, NJ), Chap. 8, pp. 407–418.
- Roberts, P. L. D., and Jaffe, J. S. (2007). "Multiple angle acoustic classification of zooplankton," *J. Acoust. Soc. Am.* **121**, 2060–2070.
- Stanton, T. K., Chu, D. Z., Wiebe, P. H., Martin, L. V., and Eastwood, R. L. (1998a). "Sound scattering by several zooplankton groups. I. Experimental determination of dominant scattering mechanisms," *J. Acoust. Soc. Am.* **103**, 225–235.
- Stanton, T. K., Chu, D. Z., and Wiebe, P. H. (1998b). "Sound scattering by several zooplankton groups. II. Scattering models," *J. Acoust. Soc. Am.* **103**, 236–253.
- Warren, J. D., Stanton, T. K., McGehee, D. E., and Chu, D. Z. (2002). "Effect of animal orientation on acoustic estimates of zooplankton properties," *IEEE J. Ocean. Eng.* **28**, 271–282.
- Wiebe, P. H., Greene, C. H., Stanton, T. K., and Burczynski, J. (1990). "Sound scattering by live zooplankton and micronekton—empirical studies with a dual-beam acoustical system," *J. Acoust. Soc. Am.* **88**, 2346–2360.